International Journal of Earth Sciences Knowledge and Applications
journal homepage: http://www.ijeska.com/index.php/ijeska
e-ISSN: 2687-5993

Research Article https://doi.org/10.5281/zenodo.18076230

Geochemistry of Alluvial Deposits in the Baboa De Kole Area (Tshopo Province, Democratic Republic of Congo): Implications for Provenance, Chemical Alteration and Tectonic Setting

Innocent Agama Badriyo[1,2]*, Christophe Kabala Imoya[3], Dimitri Elukesu Mbula[3], Philippe Essomba[4]

[1]*Goma Volcano Observatory, Department of Seismology, North-Kivu province, Democratic Republic of Congo*
[2]*Department of Geology, Faculty of Sciences and Technology, University of Goma, Goma, Democratic Republic of Congo*
[3]*Department of Geology, Faculty of Sciences, University of Kisangani, Kisangani, Democratic Republic of Congo*
[4]*Department of Geology, Faculty of Sciences, University of Yaoundé 1, Yaoundé, Cameroun*

INFORMATION

Article history
Received 04 January 2026
Accepted 26 January 2026
Published 30 April 2026

Contact
*Innocent Agama Badriyo
ibadriyo@gmail.com (IAB)
https://orcid.org/0009-0006-5065-8857

How cite
Badriyo, I.A., Imoya, C.K., Mbula, D.E., Essomba, P., 2026. Geochemistry of Alluvial Deposits in the Baboa De Kole Area (Tshopo Province, Democratic Republic of Congo): Implications for Provenance, Chemical Alteration and Tectonic Setting. *International Journal of Earth Sciences Knowledge and Applications* 8 (1), xxx-xxx. https://doi.org/10.5281/zenodo.18076230.

Abstract
The Baboa de Kole alluvial sediments (Tshopo Province, Democratic Republic of Congo) constitute a key archive for reconstructing weathering, provenance and sediment recycling in the Archean greenstone belts of Central Africa. This study integrates major- and trace-element geochemistry to evaluate chemical weathering intensity, sediment maturity, source-rock characteristics, trace-element enrichment patterns and tectonic setting. Elemental compositions obtained by energy-dispersive X-ray fluorescence (ED-XRF) reveal silica-rich assemblages dominated by quartz, together with significant TiO_2 and Fe_2O_3 contents reflecting heavy minerals and secondary iron oxides. High CIA (81–91) and PIA (> 89) values indicate intense chemical weathering under humid tropical conditions, consistent with advanced feldspar alteration and clay formation. Herron's discrimination diagram shows that most samples plot in the ferruginous sandstone field, with minor ferruginous shale–litharenite compositions, pointing to oxidative weathering typical of ferralitic soils. Provenance indicators suggest derivation mainly from mafic protoliths, combined with contributions from recycled crustal material and possible hydrothermal quartz inputs. Enrichment of Cr, V and Zr reflects the concentration of resistant heavy minerals, whereas anomalous Ag and Cd contents may be linked to sulfide phases and/or hydrothermal influence. Tectonic discrimination plots display mixed signatures between passive and active continental margin settings, implying a composite geodynamic control on sediment supply. Overall, the geochemical dataset reveals highly weathered, compositionally mature sediments sourced from variably altered mafic rocks and recycled materials, deposited under humid tropical conditions. These results provide new insights into sediment generation processes and the tectono-sedimentary evolution of alluvial systems associated with Archean greenstone terranes in Central Africa.

Keywords
Baboa de Kole, alluvial sediments, geochemistry, greenstone belt, tectonic setting

Abbreviations

CIA : Chemical Index of Alteration
PIA : Plagioclase Index of Alteration
ICV : Index of Compositional Variability

1. Introduction

Alluvial sediments play a key role in reconstructing weathering, erosion, and sediment-transport processes at the scale of drainage basins. Geochemical characterization of

major and trace elements enables identification of potential source lithologies, evaluation of compositional maturity, and inference of depositional conditions (McLennan et al., 1993; Nesbitt and Young, 1982). In Archean greenstone belts, such approaches are particularly valuable because complex tectono-metamorphic histories and strong lithological variability exert a major control on sediment composition (De Wit and Ashwal, 1997).

The Baboa de Kole area (Tshopo Province, Democratic Republic of Congo) lies within the northeastern Congo Craton, a region characterized by extensive Archean greenstone–granite terranes commonly referred to as the Bomu–Kibalian block (Turnbull et al., 2021; Cahen et al., 1984). This block encompasses several terranes, including the Bomu Amphibolite and Gneiss Complex and the West Nile Gneissic Complex, with felsic–intermediate magmatism dated between ca. 3.2 and 2.5 Ga, as constrained by recent U–Pb zircon geochronology (Turnbull et al., 2021). The northern part of this domain hosts structurally complex greenstone belts with documented gold mineralization, notably in the Moto–Kibali district (Allibone et al., 2020).

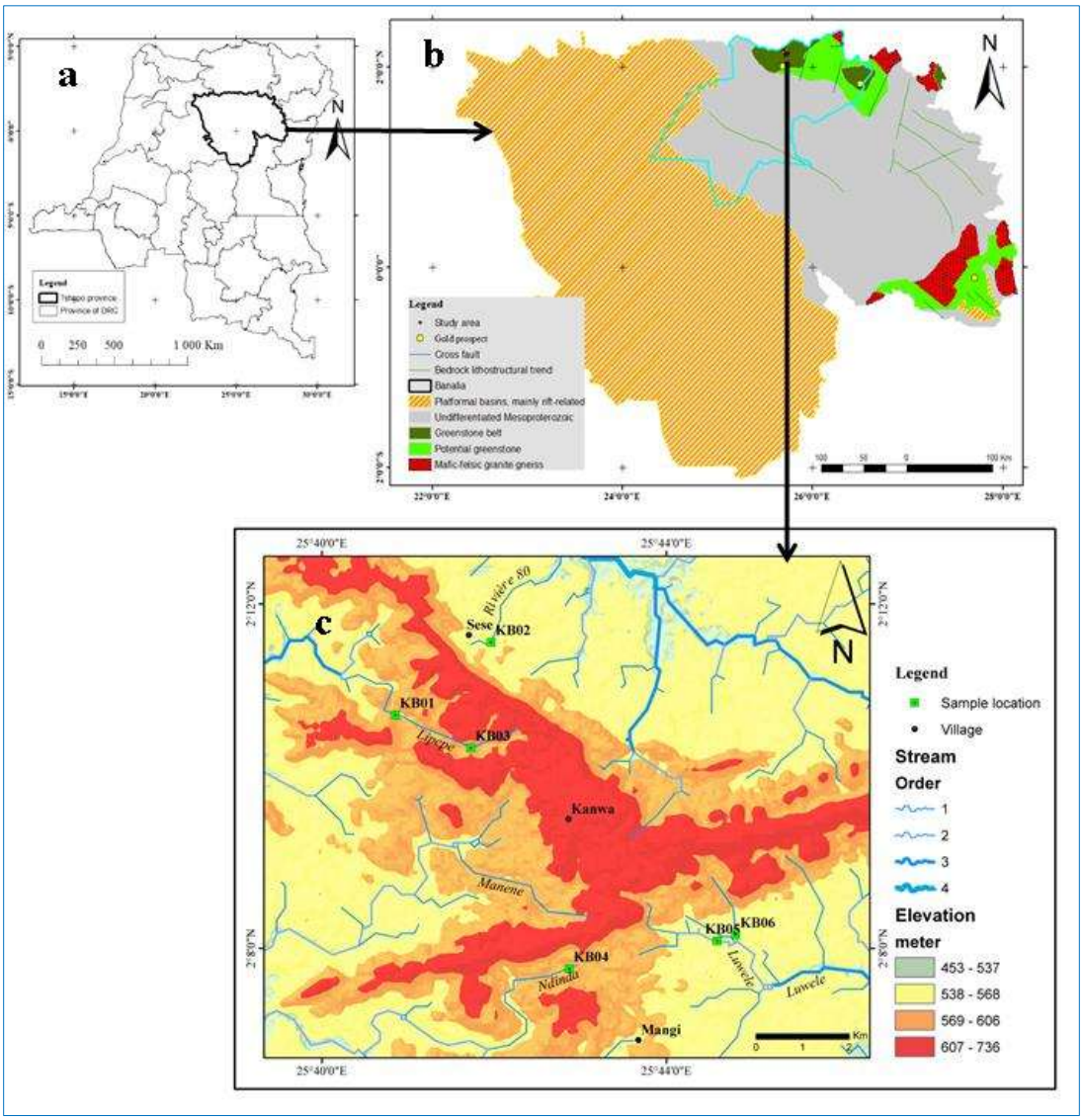

Fig. 1: a) Map of the Democratic Republic of Congo highlighting Tshopo Province in black, b) Geological map of Tshopo Province showing major geological units, with the Banalia territory highlighted in green; the arrow indicates the location of the study area (modified from Kabete et al., 2021) and c) Map of the study area showing the hydrography of the Baboa de Kole sector, elevation, and sampling locations

Despite the geological significance of the Baboa de Kole region and the increasing interest in its mineral resources, detailed geochemical investigations of its alluvial sediments remain limited. Previous studies have largely been descriptive and rarely integrate geochemical analyses with systematic interpretations of sediment provenance, weathering intensity, and tectonic setting. In this context, the combined application of major- and trace-element geochemistry, alongside weathering and sediment-maturity indices (e.g., Chemical Index of Alteration (CIA), Plagioclase Index of Alteration (PIA), Index of Compositional Variability (ICV)) and tectonic discrimination diagrams, provides a robust framework for reconstructing sediment sources and paleoenvironmental conditions (McLennan et al., 1990; Herron, 1988; Taylor and McLennan, 1985).

This study aims to (i) characterize the geochemical composition of alluvial sediments from Baboa de Kole, (ii) constrain their likely source rocks and degree of chemical weathering, and (iii) discuss the sedimentary and tectonic processes that influenced their evolution. By integrating geochemical data with the regional geological framework, this work provides new insights into sedimentary dynamics in the northeastern Congo Craton and offers a baseline for future geological, environmental, and mineral-resource assessments.

2. Geographical and Geological Setting

The Baboa de Kole area is located in Tshopo Province, northeastern Democratic Republic of Congo (DRC) (Fig. 1), in the Congo River drainage basin. The landscape is characterized by low relief, dense equatorial forest, and extensive lateritic mantles developed under persistently humid tropical conditions. High rainfall, intense leaching, and prolonged chemical weathering in tropical climates result in the removal of mobile elements and the accumulation of resistant elements in soils and sediments, as shown in lateritic profiles and geochemical studies (Braun et al., 2012; Braun et al., 2005; Tardy, 1997).

Geologically, the study area lies on the northeastern margin of the Congo Craton, within the Bomu–Kibalian terrane, one of the major Archean provinces of Central Africa. This terrane consists mainly of granitoid batholiths, greenstone belts, and gneissic complexes that record multiple episodes of magmatism, deformation, and metamorphism between ca. 3.2 and 2.5 Ga (Turnbull et al., 2021; De Wit and Ashwal, 1997; Cahen et al., 1984). Archean greenstone belts, including those of the Kibalien Superterrane, typically consist of mafic–ultramafic volcanic sequences, intercalated sediments such as banded iron formations, and are commonly intruded by tonalite–trondhjemite–granodiorite (TTG) granitoids (Kabete et al., 2021; De Wit and Ashwal, 1997; Condie, 1981).

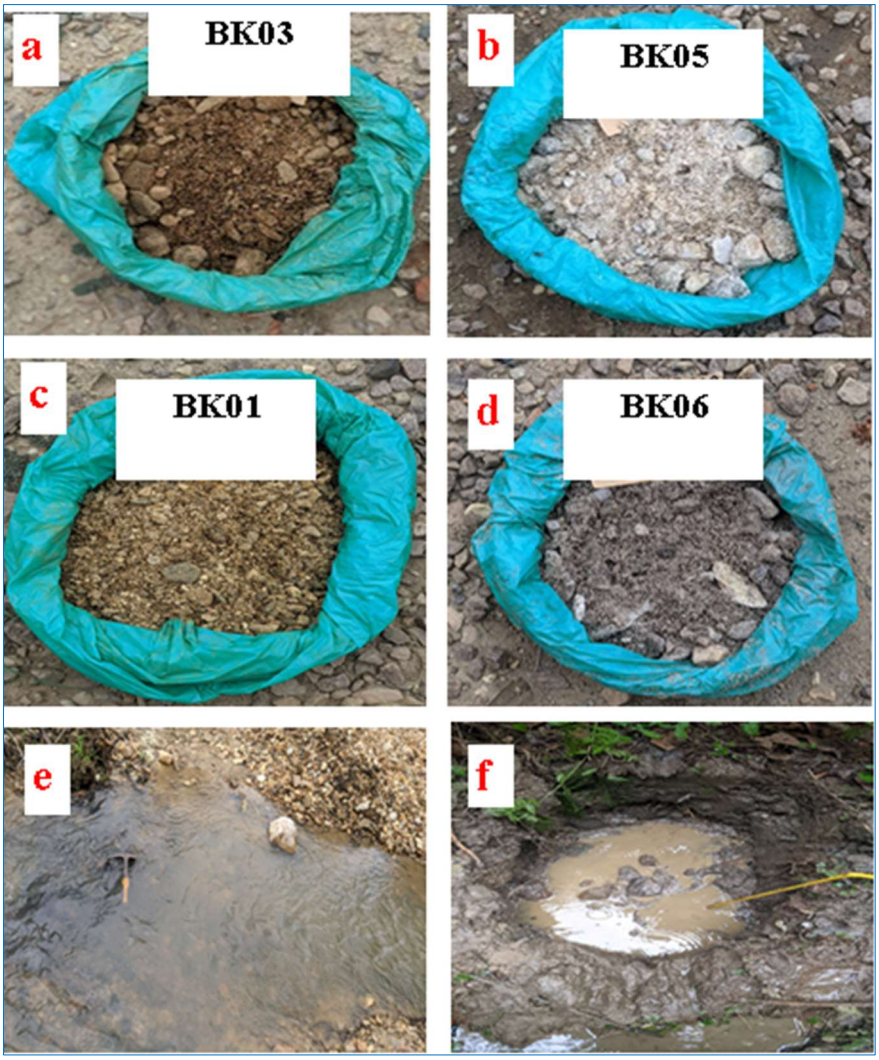

Fig. 2: a-d) Representative sediment samples from the Baboa de Kole area, e) One of the sampled stream channels and f) A small sampling pit excavated for sediment collection

The northeastern Congo Craton is well known for its mineralization potential, particularly orogenic gold deposits hosted along major shear zones and lithological contacts, as observed in the Moto–Kibali district and adjacent greenstone belts (Kabete et al., 2021; Allibone et al., 2020; Groves et al., 2010). Hydrothermal alteration associated with these systems

commonly produces quartz veins, iron oxides, and sulfide-bearing assemblages, which may contribute detrital material to surrounding sediments (Taylor and McLennan, 1985; Nesbitt and Young, 1982).

The alluvial sediments investigated here are mainly deposited along active stream channels and floodplains. They represent a mixture of materials derived from (i) in-situ weathering of Archean basement rocks, (ii) reworking of older lateritic mantles, and (iii) recycling of detritus transported from upstream areas. As such, they preserve an integrated record of lithological variability, weathering intensity, and sedimentary recycling across the catchment (McLennan et al., 1993; Cox et al., 1995).

Table 1. Major and trace-element composition of sediments from the Baboa de Kole Area

	BK01	BK02	BK03	BK04	BK05	BK06
SiO_2	81.43	75.30	19.60	60.92	84.60	82.11
TiO_2	6.13	4.98	4.96	2.30	0.69	4.08
Al_2O_3	7.27	7.08	10.70	6.40	8.01	5.40
Fe_2O_3	3.73	6.68	7.91	0.64	1.00	4.39
MnO	0.09	0.09	0.07	0.03	0.01	0.08
MgO	0.27	0.29	0.69	0.40	0.22	0.32
CaO	0.23	0.02	0.04	0.11	0.18	0.31
Na_2O	0.56	0.57	0.52	0.54	0.30	0.22
K_2O	0.11	0.13	0.09	0.18	0.02	0.31
P_2O_5	0.17	0.19	0.08	0.15	0.10	0.24
Total	100.00	95.32	44.66	71.67	95.12	97.45
LOI	0.00	4.68	55.34	28.33	4.88	2.55
Zr	10.81	0.00	0.00	20.15	0.15	13.53
Nb	1.15	0.66	0.92	0.87	1.29	0.85
Th	0.00	0.85	0.55	0.00	0.00	0.00
Pb	0.21	0.55	0.67	0.26	0.33	0.05
Sr	0.01	0.00	0.00	0.02	0.01	0.07
Nd	7.08	0.32	0.00	2.04	0.77	0.00
Cd	20.41	9.18	68.37	45.92	57.14	60.20
Sn	0.00	0.00	6.56	6.31	4.02	7.76
Zn	1.29	0.27	0.68	0.20	0.00	0.00
Y	0.96	0.00	0.34	0.43	0.36	0.35
V	0.00	60.00	0.00	0.00	0.00	0.00
Cr	133.94	5.40	7.44	0.96	1.79	16.20
Ag	0.00	197.33	0.00	146.67	160.00	0.00
Cl	262.7	338	843	299.1	223	325
SiO_2/Al_2O_3	11.20	10.64	1.83	9.52	10.56	15.21
Log (SiO_2/Al_2O_3)	1.05	1.03	0.26	0.98	1.02	1.18
Al_2O_3/TiO_2	1.19	1.42	2.16	2.78	11.64	1.33
K_2O/Na_2O	0.20	0.22	0.17	0.33	0.08	1.45
Na_2O/K_2O	4.91	4.48	5.94	3.05	13.32	0.69
Fe_2O_3/K_2O	32.59	52.72	91.02	3.62	44.71	14.00
Log (Fe_2O_3/K_2O)	1.51	1.72	1.96	0.56	1.65	1.15
Na_2O+K_2O	0.68	0.69	0.60	0.71	0.32	0.53
$Al_2O_3+Na_2O+K_2O$	7.95	7.77	11.30	7.11	8.33	5.93
Fe_2O_3+MgO	4.00	6.97	8.60	1.04	1.22	4.72
$Al_2O_3/(CaO+MgO+Na_2O+K_2O)$	6.19	7.08	8.00	5.22	11.13	4.65
DF1	-12.87	-8.86	-6.27	-9.30	-4.80	-10.29
DF2	-3.77	-5.12	-5.77	-4.92	-5.95	-5.24
CaO*	-0.0010	-0.0022	-0.0008	-0.0013	-0.0004	-0.0014
CIA	83.20	86.48	91.32	83.42	90.56	81.15
PIA	89.66	90.68	93.24	89.18	94.64	95.97
ICV	1.70	1.76	1.32	0.88	0.36	1.87
ICV = (Fe_2O_3 + K_2O + Na_2O + CaO* + MgO + TiO_2)/Al_2O_3 after Cox et al. (1995)						
CIA (%) = (Al_2O_3/(Al_2O_3+CaO* + Na_2O + K_2O)) × 100 after Nesbitt and Young (1982)						
PIA (%) = [(Al_2O_3 - K_2O)/(Al_2O_3 + CaO* + Na_2O - K_2O)] × 100 after Fedo et al. (1995)						
CaO* = ¼ CaO - 10/3 P_2O_5						

DF1 (Discriminant Function 1)=(-1.773×TiO_2%)+(0.607×Al_2O_3%)+(0.76×Fe_2O_3T%)+(-1.5×MgO%)+(0.616×CaO%)+(0.509×Na_2O%)+(-1.22×K_2O%)+(-9.09). DF2 (Discriminant Function 2) =(0.445×TiO_2%)+(0.07×Al_2O_3%)+(-0.25×Fe_2O_3T%)+(-1.142×MgO%)+(0.432×Na_2O%)+(1.426×K_2O%)+(-6.861). Major oxides are reported in weight percent (wt%), whereas trace and minor elements are expressed in parts per million (ppm).

At the regional scale, the Bomu–Kibalian terrane forms part of the broader Central African Shield and interacts structurally with the Ubendian–Usagaran and Kibaran belts that developed during Paleoproterozoic to Mesoproterozoic orogenic cycles (Tack et al., 2010; Begg et al., 2009). These large-scale tectono-magmatic events promoted exhumation and exposure of Archean crustal blocks that today constitute the main sediment sources feeding the Baboa de Kole drainage basin.

Overall, the geographical and geological framework of the Baboa de Kole area provides an appropriate natural laboratory for evaluating sediment provenance, the degree of chemical weathering, and the imprint of tectonic setting on alluvial geochemistry

3. Materials and Methods

3.1 X-ray Fluorescence Spectroscopy (ED-XRF)

The elemental composition of the samples was performed

using energy-dispersive X-ray fluorescence (ED-XRF) with a XEPOS III spectrometer at the Central Laboratory of Analyses of the Commissariat Général à l'Energie Atomique/Regional Center for Nuclear Studies of Kinshasa (CGEA/CREN-K). Samples were oven-dried, ground, and sieved to <63 µm. Pellets were prepared by mixing 5 g of powdered material with 1 g of Fluxana binder and pressing them under hydraulic pressure, following standard procedures for sediment geochemistry. Analytical conditions and quality control followed general ED-XRF protocols (Jenkins, 1999; Potts and Webb, 1992).

Measurements were carried out using the "FP-Pellets" and "TQ-Pellets Fast" analytical modes. Certified reference materials (ISE-870, ISE-890, ISE-919, ISE-961 and SOIL-7) were used to check accuracy and reproducibility throughout the analytical sequence (Costa et al., 2024; Barreto et al., 2004).

Four secondary targets (Mo, Al_2O_3, Co and HOPG) were used sequentially to optimize excitation conditions across the periodic table. Concentrations were obtained by external calibration, and uncertainties were evaluated from replicate analyses. Detection limits were typically ≤1 wt% for major oxides and lower for most trace elements, in agreement with previously reported performance ranges for ED-XRF applied to geological materials (Potts and Webb, 1992).

3.2. Weathering and Sediment Maturity Indices

Several chemical indices were calculated to evaluate the degree of source-rock weathering, sediment recycling and compositional maturity. Major oxides were recalculated on a volatile-free basis prior to computation (McLennan, 1993). The Chemical Index of Alteration (CIA) was calculated following Nesbitt and Young (1984):

$$CIA = Al_2O_3/ (Al_2O_3 + CaO^* + Na_2O + K_2O) \times 100 \text{ (molar compositions)} \quad (1)$$

where; CaO* represents only calcium hosted in silicate minerals. Carbonate- and phosphate-bound Ca was corrected using established procedures (Fedo et al., 1995).

To further constrain feldspar alteration, the Plagioclase Index of Alteration (PIA) was calculated after Fedo et al. (1997):

$$PIA = Al_2O_3/ (Al_2O_3 + CaO^* + Na_2O) \times 100 \text{ (molar compositions)} \quad (2)$$

Sediment compositional maturity was also assessed using the Index of Compositional Variability (ICV), which reflects the relative abundance of labile versus stable phases (Cox et al., 1995).

$$ICV = (Fe_2O_3 + K_2O + Na_2O + CaO + MgO + MnO + TiO_2) / TiO_2 \text{ (molar compositions)} \quad (3)$$

Together, CIA, PIA and ICV provide complementary information on weathering intensity and provenance and have been widely applied in tropical sedimentary systems (McLennan, 1993).

4. Results and Discussion

4.1 Major and Trace Element Geochemistry

Six alluvial deposit samples were collected, some of them are reported in Fig. 2. The major and traces element compositions of the Baboa de Kole alluvial sediments are summarized in Table 1.

Silica contents are high (60.9–84.6 wt.%), indicating a detrital assemblage strongly dominated by quartz. Only sample BK03 displays an anomalously low SiO_2 value (19.6 wt.%), which likely reflects a higher proportion of fine, clay-rich and/or Fe-bearing phases.

Al_2O_3 contents (5.4–12.0 wt.%) point to moderate amounts of aluminosilicate minerals, largely derived from feldspar weathering, whereas Fe_2O_3 values (0.64–7.91 wt.%) are consistent with secondary iron oxides formed during weathering and early diagenesis. The low alkali contents ($Na_2O + K_2O$ = 0.3–0.7 wt.%) suggest limited feldspar input and relatively high chemical maturity, in agreement with the high CIA values (Amiewalan et al., 2020; Nesbitt and Young, 1982).

TiO_2 concentrations range from 0.68 to 6.10 wt.%, which, although relatively high for typical siliciclastic sediments, fall within the range reported for deposits enriched in Ti-bearing heavy minerals such as rutile and ilmenite. These values indicate significant contributions from Ti-rich heavy-mineral concentrates, probably sourced from basement and mafic lithologies (Mbala Ngama et al., 2019; Nyobe et al., 2018; Tonje et al., 2014).

Trace-element data (Table 1) show high Ti abundances (13,800–36,750 ppm), except in BK05, further supporting the control exerted by Fe–Ti oxides on the heavy-mineral assemblages (Cullers, 2000). Zirconium concentrations vary widely and reach up to 4,837 ppm, reflecting zircon enrichment — a typical feature of detrital heavy-mineral suites and a useful provenance indicator (Garzanti et al., 2007; Morton and Hallsworth, 1999). The relative enrichment in V and Cr in several samples is consistent with contributions from titanomagnetite and other Fe–Ti phases commonly associated with mafic or volcanic components (Cullers, 2000). Overall, the geochemical signatures point to quartz-rich alluvial sediments derived mainly from weathered basement lithologies, with localized inputs of heavy-mineral–bearing components.

4.2. Geochemical Classification

The geochemical classification of the Baboa de Kole sediments using the $\log(SiO_2/Al_2O_3)$–$\log(Fe_2O_3/K_2O)$ discrimination diagram (after Herron, 1988) (Fig. 3) shows that most samples plot in the ferruginous sandstone field (≈ 67%), whereas the remaining ones fall within the ferruginous shale–litharenite fields (≈ 33%).

4.3. Degree of Weathering and Chemical Maturity

The SiO_2/Al_2O_3 ratio, a widely used indicator of mineralogical maturity, reflects progressive enrichment in quartz at the expense of feldspars, mafic minerals and lithic fragments (Roser et al., 1996; Potter, 1978). The values obtained (8.29–26.87), except for BK03 (1.8), suggest

progressive mineralogical maturity and strong quartz enrichment in most samples.

These values also imply quartz-rich and clay-poor assemblages, since SiO_2 is mainly hosted in quartz whereas Al_2O_3 is largely accommodated in clay minerals. Increasing SiO_2/Al_2O_3 is therefore consistent with sedimentary recycling and hydrodynamic sorting, reflecting the preferential survival and concentration of resistant quartz relative to less stable phases (Armstrong-Altrin et al., 2017; Roser and Korsch, 1988).

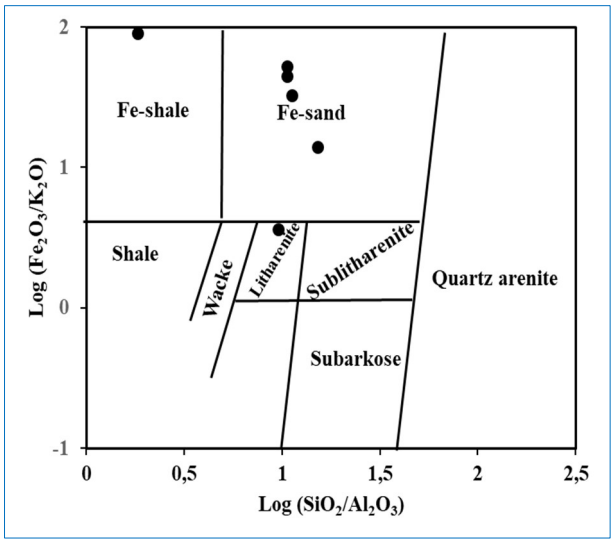

Fig. 3. Discrimination diagram Log (SiO_2/Al_2O_3) versus Log (Fe_2O_3/K_2O) (after Herron (1988)) showing that the studied alluvial sediments plot mainly in the ferruginous sandstone field, with minor occurrences in the ferruginous shale and litharenite fields

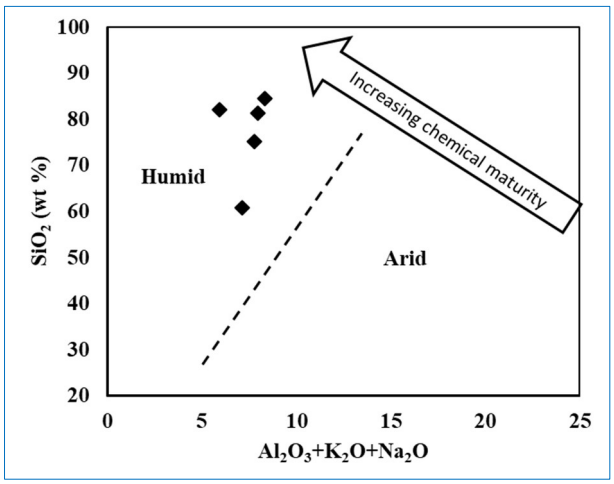

Fig. 4. SiO_2 (wt%) versus $Al_2O_3+K_2O+Na_2O$ (wt%) diagram (after Suttner and Dutta (1986)), indicating that the studied alluvial sediments were derived under humid climatic conditions and are compositionally mature

The $Al_2O_3/(CaO + MgO + Na_2O + K_2O)$ ratio ranges from 4.65 to 11.13, indicating advanced chemical weathering and preferential retention of Al in residual phases (Gill and Yemane, 1996).

The ICV ranges from 0.36 to 1.87. The lowest value in BK05 points to higher proportions of clay minerals or muscovite, whereas values close to or above 1 indicate contributions from feldspars in the source terrain (Cox et al., 1995). This implies that BK05 derived from more intensely weathered parent rocks compared with the other samples.

The CIA calculated using silicate-bound CaO (CaO*), varies between 81.15 and 91.32, suggesting intense chemical weathering commonly associated with humid climatic conditions (Mbale Ngama et al., 2019; Chen et al., 2016; Singh et al., 2005; Fedo et al., 1995). Finally, the SiO_2 versus ($Al_2O_3 + K_2O + Na_2O$) diagram (Fig. 4) after Suttner and Dutta (1986) is consistent with deposition under predominantly humid climatic conditions.

The PIA ranges from 89.18 to 95.97%, indicating intense plagioclase alteration and advanced chemical weathering of the source rocks (Fedo et al., 1997; Fedo et al., 1995).

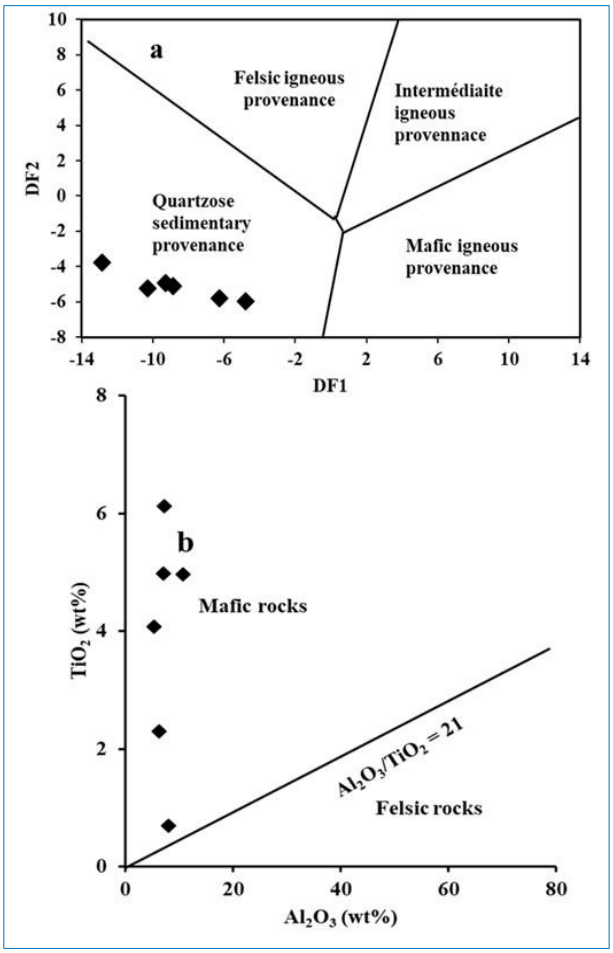

Fig. 5. Provenance discrimination diagrams: a) DF1 versus DF2 plot (after Roser and Korsch (1988)) indicating that the Baboa de Kole alluvial sediments were largely derived from recycled quartz-rich sedimentary rocks. DF1 (Discriminant Function 1) = (-1.773×TiO_2%) + (0.607×Al_2O_3%) + (0.76×Fe_2O_3T%) + (-1.5×MgO%) + (0.616×CaO%) + (0.509×Na_2O%) + (-1.22×K_2O%) + (-9.09). DF2 (Discriminant Function 2) = (0.445×TiO_2%) + (0.07×Al_2O_3%) + (-0.25×Fe_2O_3T%) + (-1.142×MgO%) + (0.432×Na_2O%) + (1.426×K_2O%) + (-6.861) and b) Al_2O_3 versus TiO_2 plot (after Hayashi et al. (1997)) suggesting additional contributions from mafic source rocks

4.4. Weathering Indices and Provenance Constraints

The DF1 versus DF2 discrimination diagram (Roser and Korsch, 1988) (Fig. 5a) places most samples in the field of

recycled quartzose sedimentary rocks, suggesting significant sediment recycling and hydrodynamic sorting, in agreement with the high quartz contents. The Al_2O_3-TiO_2 relationships (Hayashi et al., 1997) (Fig. 5b) plot predominantly within the mafic protolith field, broadly consistent with the occurrence of Archean greenstone belts in the region. However, the very high SiO_2 contents are not typical of mafic sources and may instead reflect contributions from felsic rocks and/or quartz veining, which is commonly associated with hydrothermal systems in greenstone terranes (Groves et al., 2010; McCuaig and Kerrich, 1998).

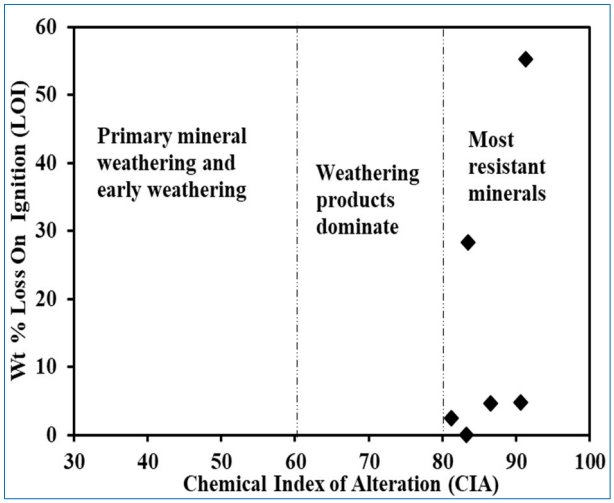

Fig. 6. LOI versus CIA plot (after Babechuck et al. (2014)) showing that the sediments are dominated by chemically resistant minerals, as reflected by CIA values exceeding 80. CIA (%) = (Al2O3/(Al2O3+CaO* + Na2O + K2O)) × 100 (after Nesbitt and Young (1982))

No systematic relationship is observed between loss on ignition (LOI) and CIA (Fig. 6). The geochemical composition indicates limited contributions from unaltered primary minerals and supports intense, prolonged chemical weathering. Sediments are dominated by resistant mineral phases, producing a mature weathering signal (Babechuk et al., 2014; Nesbitt and Young, 1982).

4.5. Degree of Trace-element Enrichment

To evaluate trace-element enrichment, the measured concentrations were normalized to Upper Continental Crust (UCC) values following the approach of Yang and Blum (1999), using the reference dataset of Taylor and McLennan (1985). This normalization allows the distinction between non-enriched, weakly enriched, and highly enriched elements relative to the average composition of the UCC (Fig. 7).

The results indicate that Zn, Y, Sr, Pb, Th and Nb display values close to those of the UCC, suggesting no significant enrichment. Sn, Cd, V, Nd and Zr show weak enrichment, probably related to the presence of resistant minerals such as zircon and monazite, as well as inherited clay phases (Wedepohl, 1995; Taylor and McLennan, 1985). In contrast, Cr, Ag and Cd exhibit pronounced enrichment.

The positive Cr anomaly implies a significant contribution from mafic to ultramafic source rocks or Cr-rich heavy minerals (e.g., chromite, titanomagnetite), whereas Ag and Cd enrichment may reflect sulfide phases and/or hydrothermal inputs associated with the source rocks (McLennan, 2001; Krauskopf and Bird, 1995). Taken together, these geochemical signatures support a mixed provenance involving mafic, sulfide phases and sedimentary units, combined with sediment recycling and selective concentration during transport and deposition.

4.6. Correlation of Major and Trace Elements

Correlation coefficients for major and trace elements are summarized in Table 2. The strong negative relationship between SiO_2 and most other oxides is consistent with a significant proportion of quartz, which tends to be mechanically stable and only weakly affected by chemical weathering (Taylor and McLennan, 1985; Nesbitt and Young, 1982).

In contrast, positive correlations among Ti, Fe, Mn and several transition metals (e.g., V, Cr) may reflect contributions from Fe–Ti oxides and ferromagnesian minerals (Duchesne and Bologne, 2009), as observed in regional surface sediments where significant positive correlations of Ti with Fe and Mn are interpreted to indicate detrital and heavy-mineral control (Selvaraj and Chen, 2006). Associations between Ti and selected high-field-strength elements likely reflect co-occurrence with resistant accessory minerals rather than simple incorporation into a single phase (McLennan, 2001).

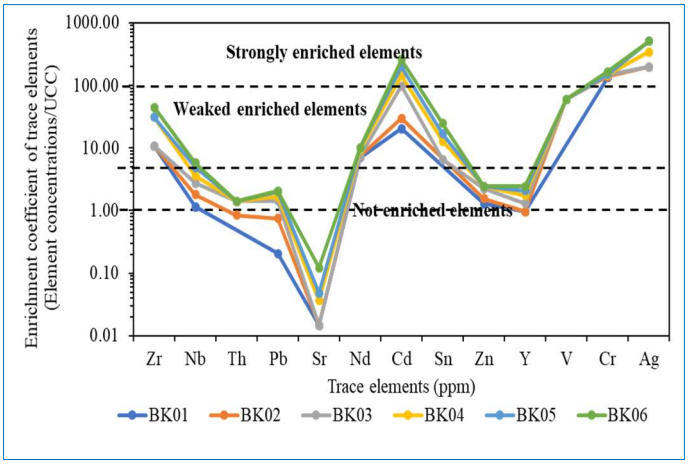

Fig. 7. Trace-element normalized patterns (after Yang and Blum (1999)) for the studied alluvial sediments, using the Upper Continental Crust values of Taylor and McLennan (1985). The diagram shows three domains: (i) non-enriched elements (Nb, Th, Pb, Sr, Zn, Y), (ii) weakly enriched elements (Nd, Sn, Zr, V), and (iii) strongly enriched elements (Cd, Cr, Ag)

Positive relationships involving Al-rich components (e.g., Al_2O_3 together with Ca, Sr or Zr) may indicate a combination of feldspar weathering and the formation of clay minerals, although part of the Zr is probably hosted by zircon (Fedo et al., 1995; Nesbitt and Young, 1984). The correlation between Al_2O_3 and REE suggests adsorption or retention within clay and other aluminosilicate phases, but multiple mineral hosts are likely (McLennan and Taylor, 1991).

Overall, these patterns point to mixed mineralogical controls

rather than single-phase behavior and should be interpreted cautiously. The observed correlations among major and trace elements likely reflect combined mineralogical and weathering controls. Positive correlations between SiO_2, CaO, and P_2O_5 suggest contributions from feldspars and apatite, potentially derived from mafic or felsic components in the source area (Fedo et al., 1995; Taylor and McLennan, 1985). Enrichments in Ti, Fe, Mn, and Cr are consistent with the presence of resistant heavy minerals and ferromagnesian phases, such as ilmenite, magnetite, and spinels, which serve as carriers of these elements in sediments (McLennan, 2001; Nesbitt and Young, 1982).

Table 2. Correlation matrix of the alluvial sediments from Baboa de Kole

	SiO_2	TiO_2	Al_2O_3	Fe_2O_3	MnO	MgO	CaO	Na_2O	K_2O	P_2O_5	V	Cr	Cu	Zn	Ag	Cl	Zr
SiO_2	1.00																
TiO_2	-0.21	1.00															
Al_2O_3	-0.78	0.12	1.00														
Fe_2O_3	-0.53	0.73	0.48	1.00													
MnO	-0.08	0.96	-0.05	0.75	1.00												
MgO	-0.98	0.25	0.70	0.55	0.13	1.00											
CaO	0.60	-0.06	-0.58	-0.41	0.00	-0.47	1.00										
Na_2O	-0.38	0.49	0.33	0.27	0.35	0.28	-0.68	1.00									
K_2O	0.19	0.22	-0.70	0.04	0.37	-0.04	0.51	-0.36	1.00								
P_2O_5	0.58	0.35	-0.85	0.04	0.54	-0.48	0.48	-0.21	0.82	1.00							
V	0.16	0.27	-0.11	0.44	0.40	-0.23	-0.56	0.38	-0.07	0.31	1.00						
Cr	0.28	0.60	-0.08	-0.01	0.49	-0.27	0.42	0.30	-0.05	0.20	-0.21	1.00					
Cu	-0.94	0.27	0.87	0.64	0.14	0.93	-0.46	0.21	-0.26	-0.61	-0.20	-0.19	1.00				
Zn	-0.20	0.77	0.31	0.32	0.59	0.18	0.05	0.57	-0.19	-0.07	-0.16	0.88	0.26	1.00			
Ag	0.29	-0.55	-0.18	-0.35	-0.47	-0.41	-0.50	0.17	-0.35	-0.09	0.59	-0.51	-0.44	-0.59	1.00		
Cl	-0.95	0.35	0.79	0.73	0.25	0.96	-0.50	0.24	-0.13	-0.48	-0.09	-0.23	0.98	0.23	-0.43	1.00	
Zr	0.21	-0.05	-0.66	-0.54	-0.06	-0.12	0.47	-0.03	0.65	0.47	-0.42	0.20	-0.42	0.03	-0.19	-0.38	1.00

Method : A correlation matrix was computed in Microsoft Excel using the Data → Data Analysis → Correlation procedure applied to the normalized dataset. The matrix was subsequently visualized using conditional formatting to enhance readability. A color scale was defined such that coefficients approaching +1 are shown in blue and those approaching 1 in red, with intermediate values represented by gradual transitions. This visualization facilitates the assessment of both the magnitude and direction of relationships among the analyzed variables

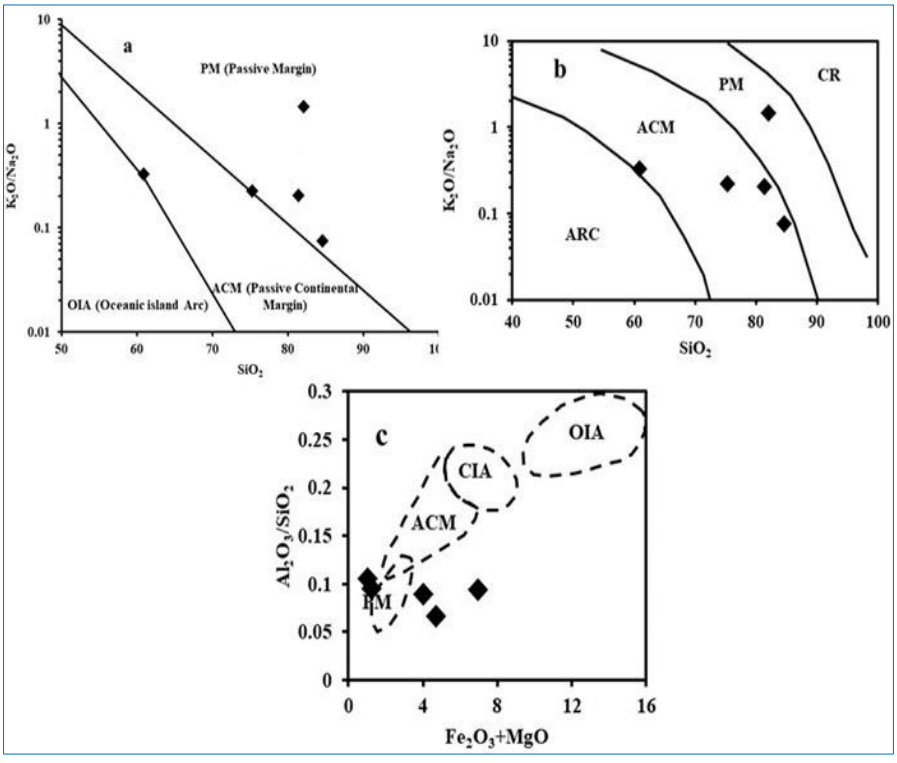

Fig. 8. Tectonic discrimination diagrams based on the major-element geochemistry of the analyzed alluvial sediments: a) SiO_2 (wt%) versus K_2O/Na_2O plot (after Roser and Korsch (1986)), showing that the sediments mainly derive from passive margins and, to a lesser extent, from active continental margins. (b) Adapted version of the SiO_2 (wt%) versus K_2O/Na_2O diagram (after Roser and Korsch (1986)), highlighting the relative contribution of active continental margin sources and c) (Fe_2O_3T+MgO) (wt%) versus Al_2O_3/SiO_2 diagram (after Bhatia (1983)), showing that the sediments plot near passive and active continental margin fields. The fields correspond to passive margins (PM), active continental margins (ACM), continental island arcs (CIA), oceanic island arcs (OIA), and continental rift settings (CR)

Al-rich clay minerals likely acted as important adsorption sites for several trace elements during weathering and diagenesis (Cox et al., 1995; McLennan and Taylor, 1991). The behavior of relatively immobile or incompatible

elements, such as Zr and REE, reflects the influence of resistant accessory minerals, while K and P behavior may be controlled by both primary mineralogy and post-depositional processes. Because many of these geochemical associations are not unique, their interpretation should be approached with caution.

Several studies have shown that intense chemical weathering in source areas results in elevated chemical alteration indices. The Chemical Index of Alteration (CIA) and Plagioclase Index of Alteration (PIA**)** are widely used to quantify weathering intensity, with values above ~75–80 % typically indicating strong weathering of source rocks (Fedo et al., 1995; McLennan et al., 1993). In weathering profiles developed on Archean granitoids, mobile elements such as Na, Ca, and Sr are progressively lost, whereas high-field-strength elements (HFSE) like Ti, Zr, and Th remain relatively immobile, resulting in their relative enrichment in highly weathered sediments (Panahi et al., 2000).

4.7. Tectonic Contexts

The mixed tectonic signal observed in the Baboa de Kole sediments, plotting between typical passive- and active-margin fields (Fig. 8), is comparable to many Precambrian and Phanerozoic siliciclastic successions worldwide. Previous studies have shown that sediment recycling and variable inputs from magmatic arcs can produce intermediate patterns on major- and trace-element discrimination diagrams, complicating simple tectonic interpretations (McLennan et al., 1990; Bhatia and Crook, 1986; Roser and Korsch, 1986; Bhatia 1983).

Many Archean and Paleoproterozoic sediments also display intense chemical weathering, reflected in high CIA and PIA values and relative enrichment in immobile elements such as Ti, Zr, and Th (Taylor and McLennan, 1995; Nesbitt and Young, 1982). In several cratonic successions, these geochemical patterns may plot between passive- and active-margin fields, although tectonic interpretations remain debated (Condie, 1993). Similar weathering-related trends have been documented in West African and Amazonian cratons, where prolonged alteration and sediment recycling dominate (Martins et al., 2004; Kroonenberg, 1994; Nahon, 1991).

Analogous tectono-sedimentary settings occur in many forelands and strike-slip basins bordering orogenic belts, where quartz-rich recycled sediments are commonly mixed with arc-derived volcanic detritus (Ingersoll, 1990; Dickinson, 1988). Such mixtures can produce intermediate geochemical signatures that sometimes plot near the boundary between passive- and active-margin fields on commonly used discrimination diagrams (Floyd et al., 1991).

In Central and East Africa, comparable mixed signatures have been interpreted in basins influenced by greenstone belts and intracratonic rifting, although the geodynamic histories are complex and remain debated (Kabete et al., 2021; De Waele et al., 2006; Kampunzu and Lubala, 1991).

Collectively, these analogues suggest that the Baboa de Kole alluvial sediments likely originated from a composite hinterland composed of (i) recycled and weathered cratonic and sedimentary units and (ii) mafic–intermediate volcanic or volcanogenic rocks related to ancient tectono-magmatic activity. This interpretation is consistent with the strong chemical weathering indices, the occurrence of resistant heavy minerals, and the influence of greenstone belts documented in the study area.

5. Conclusion

This study provides a comprehensive geochemical characterization of alluvial sediments from the Baboa de Kole area, along the northeastern margin of the Congo Craton. The sediments are compositionally mature and quartz-rich, with variable contributions of clay-rich material, reflecting progressive chemical weathering, hydraulic sorting, and sediment recycling. Weathering indices, including CIA, PIA, and ICV, indicate moderate to intense chemical alteration under warm and humid conditions, leading to the preferential loss of mobile elements and residual enrichment in stable mineral phases. Provenance analyses reveal a mixed source signature, with sediments derived from both mafic–intermediate greenstone-belt lithologies and highly weathered Archean granitoid and gneissic crust. Trace-element patterns and tectonic discrimination diagrams suggest that these sediments record contributions from both recycled cratonic material and arc-derived volcanic sources. The observed geochemical signatures also reflect the influence of prolonged tropical weathering and repeated fluvial reworking, highlighting the complex interplay of provenance, weathering, and sediment transport in shaping the alluvial deposits. Overall, the results establish a geochemical baseline for the Baboa de Kole alluvial system and provide new insights into the weathering processes, sedimentary recycling, and landscape evolution of Archean terranes. Future studies incorporating mineralogical and isotopic analyses, along with broader spatial sampling, will further refine source-area reconstructions and improve our understanding of trace and heavy element mobility in auriferous alluvial environments.

Acknowledgements

The authors gratefully acknowledge the staff of the Central Laboratory of Analyses of the *Commissariat Général à l'Énergie Atomique/Regional Center for Nuclear Studies of Kinshasa* (CGEA/CREN-K) for carrying out the geochemical analyses. The authors also express their sincere appreciation to the authorities of the Faculty of Sciences of the University of Kisangani for issuing the research authorization letters, as well as to the civil and military authorities of the Baboa De Kole community for their support and cooperation during the fieldwork. The authors further thank colleagues for their constructive suggestions, which contributed to improving the quality of this manuscript. This research received no external funding, and all analytical costs were covered by the authors. The authors declare that they have no conflicts of interest. Any remaining errors are the sole responsibility of the authors.

Privacy Statement

The names and email addresses provided on the journal's submission platform will be used exclusively for the purposes of managing the manuscript and publication process. They will not be shared with any third party or used for any other purpose.

References

Allibone, AH, Vargas, C, Mwandale, E, Kwibisa, J, Jongens, R, Quick, S, Komarnisky, N., Fanning, M., Bird, P., MacKenzie, D., Turnbull, R., Holliday, J., 2020. Orogenic gold deposits of the Kibali district, Neoarchean Moto Belt, northeastern Democratic Republic of Congo. In: Sillitoe RH, Goldfarb RJ, Robert F, Simmons SF, eds. Geology of the World's Major Gold Deposits and Provinces. Society of Economic Geologists 185-201. http://doi.org/10.5382/SP.23.09.

Amiewalan, F.O., Balogun, F.O., Ejairu, K., 2020. Sedimentological and geochemical characterization of DF-2 well, onshore western Niger Delta: implications for provenance, tectonic history and paleo depositional conditions. Global Journal of Pure and Applied Sciences 26, 141-155. https://doi.org/10.4314/gjpas.v26i2.6.

Armstrong-Altrin, J.S., Lee, Y.I., Kasper Zubillaga, J.J., Trejo Ramírez, E., 2017. Mineralogy and geochemistry of sands along the Manzanillo and El Carrizal beach areas, southern Mexico: implications for palaeoweathering, provenance, and tectonic setting. Geological Journal 52 (4), 559-582. https://doi.org/10.1002/gj.2792.

Babechuk, M.G., Stern, R.A., Moyen, J.F., Martin, H., 2014. Provenance and tectonic setting of Neoarchean sandstones from the Abitibi subprovince, Canada: Implications for early crustal evolution. Precambrian Research 253, 200-218. https://doi.org/10.1016/j.precamres.2014.08.013.

Barreto, S.R.G., Nozaki, J., De Oliveira, E., Do Nascimento Filho, V.F., Aragão, P.H.A., Scarminio, I.S., Barreto, W.J., 2004. Comparison of metal analysis in sediments using EDXRF and ICP-OES with the HCl and Tessie extraction methods. Talanta 64, 345-354. https://doi.org/10.1016/j.talanta.2004.02.022.

Begg, G.C., Griffin, W.L., Natapov, L.M., O'Reilly, S.Y., Grand, S.P., O'Neill, C.J., Hronsky, J.M.A., Djomani, Y.P., Swain, C.J., Deen, T., Bowden, P., 2009. The lithospheric architecture of Africa: Seismic tomography, mantle petrology, and tectonic evolution. Geosphere 5 (1), 23-50. https://doi.org/10.1130/GES00179.1.

Bhatia, M.R., 1983. Plate tectonics and geochemical composition of sandstones. Journal of Geology 91, 611-627. https://doi.org/10.1086/628815.

Bhatia, M.R., Crook, K.A.W., 1986. Trace element characteristics of graywackes and tectonic setting discrimination of sedimentary basins. Contributions to Mineralogy and Petrology 92, 181-193. https://doi.org/10.1007/BF00375292.

Braun, J.J., Marechal, J.C., Riotte, J., Boeglin, J.L., Bedimo Bedimo, J.P., Ndam Ngoupayou, J.R., Nyeck, B., Robain, H., Sekhar, M., Audry, S., Viers, J., 2012. Elemental weathering fluxes and saprolite production rate in a Central African lateritic terrain (Nsimi, South Cameroon). Geochim Cosmochim Acta 99, 243-270. http://doi.org/10.1016/j.gca.2012.09.024.

Chen, J., Chen, Y., Liu, L., Ji, J., Balsam, W., 2016. Chemical weathering intensity and climate control in subtropical China inferred from river sediments. Chemical Geology 421, 44-55.

Cahen, L., Snelling, N.J., Delhal, J., Vail, J.R., Bonhomme, M., Ledent, D., 1984. The Geochronology and Evolution of Africa. Oxford: Clarendon Press; 1984. 512 p. ISBN 0 19 857544 0.

Condie, K.C., 1981.Archean Greenstone Belts. Amsterdam: Elsevier; 1981. ISBN 0444418547.

Condie, K.C., 1993. Chemical composition and evolution of the upper continental crust: Contrasts with the lower crust and mantle and Proterozoic vs. Archean crustal rocks Chemical Geology 104, 1-37. https://doi.org/10.1016/0009-2541(93)90055-2.

Costa, C., Lia, F., Sinagra, E., 2024. Seasonal and spatial discrimination of sandy beaches using energy-dispersive X-ray fluorescence spectroscopy analysis: A comparative study of Maltese bays. Environments 11, 299. https://doi.org/10.3390/environments11120299.

Cox, R., Lowe, D.R., Cullers, R.L., 1995. The influence of sedimentary recycling and basement composition on the major and trace element chemistry of sedimentary rocks. Geochimica et Cosmochimica Acta 59, 3043-3053. https://doi.org/10.1016/0016-7037(95)00240-4.

Cullers, RL., 2000. The geochemistry of shales, siltstones and sandstones of Pennsylvanian–Permian age, Colorado, USA: implications for provenance and metamorphic studies. Lithos 51 (3), 181-203. https://doi.org/10.1016/S0024-4937(99)00063-8.

De Waele, B., Cesar, M.F., Ribeiro, J.L., 2006. Greenstone-belt influence on sedimentation and tectonics in the Congo Craton. Precambrian Research 146, 188-210. https://doi.org/10.1016/j.precamres.2006.01.010.

De Wit, M.J., Ashwal, L.D., 1997. Greenstone Belts. Oxford Monographs on Geology and Geophysics No. 35. Oxford: Clarendon Press; 1997. 809 p.

Dickinson, W.R., 1988. Interpreting provenance relations from detrital modes of sandstones. In: Miall AD, ed. Provenance of Arenites. London: Geological Society, Special Publication 333-361.

Duchesne, J.C., Bologne, G., 2009. XRF major and trace element determination in Fe-Ti oxide minerals. Geologica Belgica 12 (3-4), 205-212.

Fedo, C.M., Nesbitt, H.W., Young, G.M., 1995. Unravelling the effects of potassium metasomatism in sedimentary rocks and paleosols, with implications for paleoweathering conditions and provenance. Geology 23 (10), 921-924.

Fedo, C.M., Nesbitt, H.W., Young, G.M., 1997. Plagioclase weathering and the interpretation of bulk sediment geochemistry. Journal of Geology 25 (7), 923-926.

Floyd, P.A., Sima, A., Abia, M., 1991. Geochemical evidence for recycled and mixed provenance sediments: Implications for tectonic discrimination diagrams. Sedimentary Geology 73, 235-249.

Garzanti, E, Andò, S, Vezzoli, G., 2007. Heavy-mineral concentration in modern sands: implications for provenance interpretation. In: Mange MA, Wright DT, eds. Heavy Minerals in Use: Developments in Sedimentology 58, 215-245. https://doi.org/10.1016/S0070-4571(07)58020-9.

Gill, S., Yemane, K., 1996. Implications of a Lower Pennsylvanian Ultisol for equatorial Pangean climates and early oligotrophic forest ecosystems. Journal of Geology 24 (10), 905-908.

Groves, D.I., Goldfarb, R.J., Gebre Mariam, M., Hagemann, S.G., Robert, F., 2010. Orogenic gold systems: A global perspective. Geological Society of London Special Publication.

Hayashi, K., Fujisawa, H., Holland, H.D., Ohmoto, H., 1997. Geochemistry of sedimentary rocks from northeastern Labrador, Canada. Geochim Cosmochim Acta 61, 4115-1437.

Herron, M.M., 1988. Geochemical classification of terrigenous sands and shales from core or log data. Journal of Sedimentary Petrology 58, 820-829. http://doi.org/10.1306/212F8D24-2B24-11D7-8648000102C1865D .

Ingersoll, R.V., 1990. Provenance signatures of sandstone–mudstone suites determined using assemblages of sandstone types. Journal of Sediment Petrology 60, 22-32.

Jenkins, R., 1999. X-ray Fluorescence Spectrometry, 2nd ed. Wiley, New York, 6. https://doi.org/10.1002/9781118521014.

Kabete, J.P., Mwero, B.N., Burger, G.H., 2021. Geochemical and isotopic constraints on provenance and tectonic setting of sediments in East African basins. Journal of African Earth Sciences 182, 104243. http://doi.org/10.1016/j.jafrearsci.2021.104243.

Kampunzu, AB, Lubala, RT., 1991. Organic geochemistry and hydrocarbon potential of sediments in the Congo Basin. Berlin: Springer.

Krauskopf, K.B., Bird, D.K., 1995. Introduction to Geochemistry, 4th ed. New York: McGraw-Hill.

Kroonenberg, S.B., 1994. Geochemistry of siliciclastic sediments and tectonic setting. In: Roberts AR, Edmunds MP, eds. Provenance of Arenites. London: Geological Society, London, Special Publications 135-156.

Martins, L.A., Fett, W., Oliveira, E.P., 2004. Geochemistry and provenance of Amazon Fan sediments. Marine Geology 211.

Mbale Ngama, E., Sababa, E., Bayiga, E.C., Ekoa Bessa, A.Z., Ndjigui, P-D., Bilong, P., 2019. Mineralogical and geochemical characterization of the unconsolidated sands from the Mefou River terrace, Yaoundé area, Southern Cameroon. Journal of African Earth Sciences 159, 103570. https://doi.org/10.1016/j.jafrearsci.2019.103570.

McCuaig, T.C., Kerrich, R., 1998. Evolution of Archean hydrothermal systems: evidence from greenstone belts. Economic Geology 93 (5), 827-847.

McLennan, SM., 1993. Weathering and global denudation. Journal of Geology 101 (2), 295-303. https://doi.org/10.1086/648221.

McLennan, S.M., 2001. Relationships between the trace element composition of sedimentary rocks and upper continental crust. Geochemistry, Geophysics, Geosystems 2 (4), 1020. https://doi.org/10.1029/2000GC000109.

McLennan, S.M., Hemming, S., McDaniel, D.K., Hanson, G.N., 1993. Geochemical Approaches to Sedimentation, Provenance and Tectonics. In: Johnsson, M.J. and Basu, A., Eds., Processes Controlling the Composition of Clastic Sediments: Geological Society of America, Special Papers 285, 21-40. http://doi.org/10.1130/SPE284-p21.

McLennan, S.M., Taylor, S.R., 1991. Sedimentary rocks and crustal evolution: Tectonic setting and geochemical composition. Journal of Geology 99, 535-547. https://doi.org/10.1086/629618.

McLennan, S.M., Taylor, S.R., McCulloch, M.T., 1990. Geochemical approaches to sedimentation, provenance, and tectonics. Journal Geology 98, 499-514. http://doi.org/10.1086/628815.

Morton, A.C., Hallsworth, C.R., 1999. Processes controlling the composition of heavy mineral assemblages in sandstones. Sedimentary Geology 124 (1-4), 3-29. https://doi.org/10.1016/S0037-0738(98)00118-3.

Nahon, D., 1991. Petrogenesis of laterites and bauxites. Geological Society, London, Special Publications 55, 1-59.

Nesbitt, H.W., Young, G.M., 1984. Prediction of some weathering trends of plutonic and volcanic rocks based on thermodynamic and kinetic considerations. Geochim Cosmochim Acta 48 (7), 1523-1534. https://doi.org/10.1016/0016-7037(84)90408-3.

Nesbitt, H.W., Young, G.M., 1982. Early Proterozoic climates and plate motions inferred from major-element chemistry of lutites. Nature 299, 715-717. http://doi.org/10.1038/299715a0.

Nyobe, J.M., Sababa, E., Bayiga, E.C., Ndjigui, P-D., 2018. Mineralogical and geochemical features of alluvial sediments from the Lobo watershed (Southern Cameroon): implications for rutile exploration. Comptes Rendus Geoscience 350, 119-129.

Panahi, F., Azizi, H., Mehrabi, B., 2000. Geochemistry of Archean granitoid weathering profiles: Implications for immobile element behavior. Chemical Geology 169, 77-92. https://doi.org/10.1016/S0024-4937(00)00163-5.

Potter, PE., 1978. Petrology and chemistry of modern big river sands. Journal of Geology 86 (4), 423-449.

Potts, P.J., Webb, P.C., 1992. X-ray fluorescence spectrometry in geochemical exploration. J Geochem Explor. 1992;44:251–296. https://doi.org/10.1016/0375-6742(92)90051-G.

Roser, B.P., Cooper, R.A., Nathan, S., Tulloch, AJ., 1996. Reconnaissance sandstone geochemistry, provenance, and tectonic setting of the lower Paleozoic terrains of the West Coast and Nelson, New Zealand. New Zealand Journal of Geology and Geophysics 39, 1-16.

Roser, B.P., Korsch, R.J., 1986. Determination of tectonic setting of sandstones using discriminant function analysis of major-element data. Journal of Geology 94, 635-650.

Roser, B.P., Korsch, RJ., 1988. Provenance signatures of siliciclastic sediments — Review and petrographic perspectives. Journal of Geology 96 (5), 635-655.

Selvaraj, K., Chen, C-T.A., 2006. Moderate chemical weathering of subtropical Taiwan: Constraints from solid-phase geochemistry of sediments and sedimentary rocks. Journal of Geology 114 (1), 101-116. https://doi.org/10.1086/498102.

Singh, P., Rajamani, V., Ludwig, K.R., 2005. Provenance and weathering history of Himalayan sediments: geochemical and Nd-Sr isotopic evidence from the Ganga River sediments. Sedimentary Geology 172, 47-65.

Suttner, L.J., Dutta, P.K., 1986. Alluvial sandstone composition and paleoclimate, I. Framework mineralogy. Journal of Sedimentary Petrology 56 (3), 329-345.

Tack, L., Wingate, M.T.D., De Waele, B., Meert, J., Belousova, E., Griffin, B., Tahon, A., Fernandez-Alonso, M., 2010. The 1375 Ma “Kibaran event” in Central Africa: Prominent emplacement of bimodal magmatism under extensional regime. Precambrian Research 180 (1-2), 63–84. https://doi.org/10.1016/j.precamres.2010.02.022.

Tardy, Y., 1997. Geochemistry of laterites, soils and weathering profiles. Amsterdam: Elsevier; 1997. Developments in Earth Surface Processes, Vol. 5.

Taylor, S.R., McLennan, S.M., 1985. The Continental Crust: Its Composition and Evolution. Oxford: Blackwell Scientific Publications.

Tonje, J.C., Ndjigui, P.D., Nyeck, B., Bilong, P., 2014. Geochemical features of the Matomb alluvial rutile from the Neoproterozoic Pan-African belt, southern Cameroon. Geochemistry 74 (4), 557-570. https://doi.org/10.1016/j.chemer.2013.09.002.

Turnbull, R.E., Allibone, A.H., Matheys, F., Fanning, C.M., Kasereka, E., Kabete, J., McNaughton, N.J., Mwandale, E., Holliday, J., 2021. Geology and geochronology of the Archean plutonic rocks in the northeast Democratic Republic of Congo. Precambrian Research 358, 106133. http://doi.org/10.1016/j.precamres.2021.106133.

Wedepohl, KH., 1995. The composition of the continental crust. Geochim Cosmochim Acta 59 (7), 1217-1232. https://doi.org/10.1016/0016-7037(95)00038-2.

Yang, Z., Blum, J.D., 1999. Geochemistry of heavy minerals in sandstones: Implications for provenance and chemical weathering. Chemical Geology 160, 33-44. https://doi.org/10.1016/S0009-2541(99)00088-1.